

N83 19235 04

FREE YAW PERFORMANCE OF THE MOD-0 LARGE HORIZONTAL AXIS 100 KW WIND TURBINE

R. D. Corrigan and L. A. Viterna

National Aeronautics and Space Administration
Lewis Research Center
Cleveland, Ohio 44135

ABSTRACT

The NASA Mod-0 Large Horizontal Axis 100 kW Wind Turbine was operated in free yaw with an uncone teetered, downwind rotor mounted on a nacelle having 8-1/2° tilt. Two series of tests were run, the first series with 19 meter twisted aluminum blades and the second series with 19 meter untwisted steel spar blades with tip control. Rotor speed were nominally 20, 26 and 31 rpm. It was found the nacelle stabilized in free yaw at a yaw angle of between -55° to -45°, was relatively independent of wind speed and was well damped to short term variations in wind direction. Power output of the wind turbine in free yaw, aligned at a large yaw angle, was considerably less than that if the wind turbine were aligned with the wind. For the Mod-0 wind turbine at 26 rpm, the MOSTAB computer code calculations of the free yaw alignment angle and power output compare reasonably well with experimental data. MOSTAB calculations indicate that elimination of tilt and adding coning will improve wind turbine alignment with the wind and that wind shear has a slight detrimental effect on the free yaw alignment angle.

INTRODUCTION

Free yaw of a wind turbine has been a goal of designers for some time because of the attractiveness of eliminating the yaw drive. If a wind turbine in free yaw, aligns closely with the wind direction, power output can be maximized. Additionally, an active yaw control system is not required; which simplifies control systems and reduces mechanical components. Also, it is anticipated that during shutdown in high winds, the wind turbine could be placed in free yaw with one blade tip feathered. This configuration will cause it to weather vane, bringing the blades parallel to the wind and thus reducing blade and tower loads in high winds. To be practical, a wind turbine in free yaw must align itself closely with the wind in order to allow the rotor to capture the most energy from the wind. As expected, the

power output of a wind turbine in free yaw aligned at some large yaw angle off the wind should not produce as much power compared to the wind turbine in active yaw aligned with the wind.

Tests have been conducted by NASA on free yaw of the Mod-0 wind turbine. This intermediate report will present data on the operational characteristics of the NASA Mod-0 wind turbine in free yaw having a nacelle tilt of 8.5° , 0° coning and a downwind rotor. Two blade configurations were used: (1) fixed pitch twisted aluminum blades at nominal rotor speeds of 20, 26, and 31 rpm, and (2) untwisted steel spar blades with tip control at a nominal rotor speed of 31 rpm. Operational characteristics to be presented are nacelle yaw alignment, nacelle yaw response, and power output. Experimental data for the twisted aluminum blades on nacelle yaw alignment were compared with MOSTAB computer program predictions, and MOSTAB calculations used to analyze the affects of nacelle tilt, blade coning and wind shear on Mod-0 wind turbine free yaw alignment angle.

EXPERIMENT DESCRIPTION

Free yaw tests were conducted on the NASA Mod-0 100 kW Experimental Wind Turbine, as described in References 1, 2 and 3. The wind turbine was configured with a teetered, downwind rotor. Two test series conducted, the first was with fixed pitch, twisted blades operated at nominal rotor speeds of 20, 26 and 31 rpm; and the second series with a tip-controlled blade having no twist operated at a nominal rotor speed of 31 rpm.

The Mod-0 wind turbine (Figure 1) is composed of a 31.5 meter truss tower supporting a nacelle (Figure 2) which houses the alternator, drive train assembly, yaw drive assembly and rotor assembly. In order to provide adequate clearance of the tower by the blades, the nacelle is mounted with its longitudinal axis tilted 8.5° to the horizon, rotor end elevated.

The yaw drive assembly shown in Figure 2 consists of a single hydraulic motor/gear reducer system connected through a clutch to the pinion and ring gears. For active yaw, the yaw control system was operated with the clutch engaged and the yaw brake pressurized to maintain a set nacelle yaw angle with respect to the wind. For free yaw, the yaw drive system was disengaged from the ring gear by the clutch and the yaw brake was deactivated, allowing the nacelle to move freely about the yaw axis. (The friction torque in yaw, with the yaw drive and yaw brake disengaged is estimated to be 1912 n-m based on a friction coefficient of .02, nacelle/rotor weight of 14215 Kg, and a bearing radius of .69 m.)

The rotor assembly consisted of a two bladed teetered hub with $\pm 6.0^{\circ}$ of teeter motion and 0° coning. The first series of tests were conducted with fixed pitch, twisted aluminum blades described in Table 1 and Figures 3, 4, 5. The 19.25 meter blades

TABLE 1

BLADE CHARACTERISTICS OF THE TWISTED ALUMINUM BLADES

Rotor dia., m (ft.)	38.5 (126.27)
Root cutout, % span	5
Fixed pitch	--
Blade pitch 75% span, deg	2.8
Airfoil (root to tip)	NACA 230 series
Taper	Linear
Twist, deg	26.5
Solidity	0.30
Precone, deg	0.0
Max teeter motion, deg	+6
Blade mass, kg (lb.)	1043 (2300)

TABLE 2

BLADE CHARACTERISTICS OF THE STEEL SPAR, TIP CONTROLLED BLADES

Rotor dia., m (ft.)	38.39 (126.0)
Root cutout, % span	23
Tip control, % span	30
Blade pitch, inb'd sec., deg	Zero
Airfoil (inb'd sect.)	NACA 23024
(outb'd 30%)	NACA 64 ₃ -618
Taper	Linear
Twist, deg	Zero
Solidity	0.033
Precone, deg	Zero
Max. teeter motion, deg	+6
Blade mass, kg (lb.)	1815 (4000)

have a NACA 230 series airfoil, 30° of twist and are mounted on the hub so as to have a pitch angle of $+2.8$ relative to the plane of rotation (-90° is feathered) at the .75 radius station (Figure 4). The second series of tests were conducted with untwisted steel spar, tip-controlled blades described in Table 2 and Figure 6. The 19.18 meter blades have a NACA 230 series airfoil over the inboard section and a NACA 64 series airfoil over the outboard 30%. The blade is mounted with the chord plane parallel to the plane of rotation and the tip section mounted so as to have a 0° pitch angle when parallel to the blade chord. The tips can be pitched $+10^\circ$ to -65° .

Meteorological data was taken using an array of meteorological towers 59.4 meter from the wind turbine and spaced 45° apart. For a given test, the wind data was taken from the tower most nearly upwind of the wind turbine. The sensors on the towers are mounted at the wind turbine hub height. The nacelle yaw angle shown in Figure 7, was taken as the difference between nacelle azimuth and wind azimuth taken from the performance array. Data collection and reduction was accomplished using the data system and analysis described in reference 4. Brush strip chart recordings was also used.

The Modular Stability-High Frequency Wind Energy System Version (MOSTAB-HFW) computer program, which calculates wind turbine loads and motions, was utilized to predict the wind turbine's free yaw alignment angle for comparison with experimental data. References 5, 6 and 7 describe in detail the development and use of MOSTAB-HFW. For this paper, the wind turbine with fixed pitch, twisted aluminum blades was modeled for use with the MOSTAB-HFW code as described in Appendix A. Calculations were made for various trim conditions in order to obtain a relationship between yaw torque and yaw angle, for wind speeds of 5, 7 and 9 m/s. This data was then used for the yaw angle predictions. MOSTAB calculations were then made to determine the effects of nacelle tilt, rotor coning and wind shear on the free yaw alignment of the Mod-0 wind turbine.

RESULTS

Free yaw data was collected on the rotor operating with: fixed pitch twisted aluminum blades at nominal rotor speeds of 20, 26 and 31 rpm in wind speeds of 4 to 10 m/s; and with tip-controlled steel spar blades at a rotor speed of 31 rpm in wind speeds of 4-10 m/s. The tests were designed to define wind turbine stability and performance in free yaw. Specifically, the data analysis determined the free yaw alignment angle, nacelle response to wind speed and direction changes and alternator power.

Analysis of the test data was accomplished by the use of the Bins analysis techniques (Ref. 4).

The nacelle's tilt of $8-1/2^\circ$ plays an important part in the wind turbine's free yaw alignment angle. The $8-1/2^\circ$ tilt introduces a

torque component from the rotor torque in the yaw axis. Because of the blade rotational direction and the fact the rotor is producing a torque, this torque component tends to yaw the machine in the minus yaw direction. This causes the wind turbine to align itself further away from the wind direction than if there were no tilt.

Twisted Aluminum Blades

Measured data for nacelle yaw alignment of the wind turbine in free yaw with fixed pitch twisted aluminum blades is shown in Figures 8, 9 and 10 for rotor speeds of 20, 26, and 31 rpm. The figures describe wind turbine's yaw angle, or alignment relative to the wind, wind speed distribution and yaw angle distribution when stabilized in free yaw alignment. Shown in figures 8(a), 9(a) and 10(a) for the three rotor speeds, the nacelle's yaw angle is relatively constant and independent of the wind speed. The difference in free yaw operations for the three rotor speeds is the free yaw alignment angle. This is seen from the yaw angle distribution in figures 8(b), 9(b) and 10(b) which indicates that the modal (most occurring) yaw angle of the wind turbine at 20 rpm is -46.2° , 26 rpm is -53.6° and 31 rpm is -45.4° off the wind.

The directional response of the Mod-0 wind turbine with fixed pitch, twisted aluminum blades was very stable and well damped in free yaw. The characteristics were similar for the three rotor speeds of 20, 26 and 31 rpm. Because of the similarity in directional response at the various speeds only 26 rpm rotor speed data is presented in figures 11 and 12.

These figures are segments of strip chart recordings of the nacelle azimuth, nacelle wind speed and nacelle yaw angle. The nacelle wind speed and yaw angle are measured by an anemometer/wind vane mounted 3.4 meters above the nacelle and 4.6 meters upwind of the rotor. Special care should be taken in directly using the nacelle wind speed and nacelle yaw angle in these recordings because the sensor readings of the nacelle mounted anemometer/wind vane may differ from the undisturbed wind speed and direction due to aerodynamic effects of the nacelle and rotor. As described before, the nacelle azimuth is the absolute angle of the nacelle with respect to the earth and the yaw angle is the difference between nacelle azimuth and the wind direction. The nacelle azimuth signal shows the motion of the nacelle with respect to the earth. Since the nacelle motion is generally steady, any short term fluctuations in the yaw angle signal are due mainly to wind direction variations.

Figure 11 shows the yaw response of the wind turbine operating at 26 rpm. In this case the nacelle was in active yaw aligned with the wind and then placed in free yaw. The nacelle yaw angle indicates that the nacelle yaw angle asymptotically approaches the free yaw alignment angle, with the yawing rate dependent upon the angular separation of the nacelle direction to its free yaw alignment angle and decaying to 0 as the free yaw alignment was approached. It should be noted that the nacelle's motion, as shown by nacelle

azimuth, in reaching free yaw alignment was smooth, gentle and without overshoot, indicating that the damping in yaw is very high. With a wind speed of 4 m/s, the nacelle had a 2/3 time constant (time to achieve 2/3 of the difference between an initial condition and final condition, used to describe asymptotic type situation) of approximately 30 seconds to travel from 0° yaw angle to -36° yaw angle; based on free yaw alignment of -54° yaw angle.

Once free yaw alignment has been established, nacelle yaw response to short term variations ($\pm 10^\circ$ in 10 seconds) wind direction appears well damped and stable at the three rotor speeds tested. This can be seen in figure 12 by comparing the nacelle azimuth behavior to the nacelle yaw angle behavior. Nacelle yaw angle signal shows that short term variations of $\pm 10^\circ$ or more, due to variations in wind direction, have little affect on the nacelle's motion relative to the earth.

Alternator power output for the wind turbine with twisted blades at free yaw alignment was recorded for rotor speeds of 20, 26 and 31 rpm and in wind speeds of 4 to 8 m/s. The power generating system consisted of a synchronous generator set up as shown in figure 2. For all three rotor speeds, the alternator power for the wind turbine, stabilized in free yaw, was between 30% - 50% of the alternator power for the same configuration aligned with the wind. No general relationship between power loss and yaw angle could be determined that was consistent with the data for all three rotor speeds. Since wind turbine operations at these poor efficiencies is not practical, only one power curve, typical of the three rotor speeds is shown. Figure 13 compares the power output versus wind speed, of the wind turbine at 20 rpm in active yaw aligned with the wind and in free yaw. Table 3 is a tabulation of points off the figure for the prevalent wind speeds.

TABLE 3 - WIND TURBINE PERFORMANCE - FREE YAW VS. ACTIVE YAW
INTO WIND-TWISTED ALUMINUM BLADES - 20 RPM

REF. WIND SPEED (m/s)	AT POWER- FREE YAW (kW)	YAW ANGLE- FREE YAW (DEG.)	ALT. POWER ACTIVE YAW (kW)
4	6.5	-45	15.0
5	14.0	-46	28.0
6	19.5	-46	35.0

Steel Spar Blades with Tip Control

Nacelle yaw alignment for the wind turbine in free yaw having untwisted steel spar blades with tip control is shown in figure 14 for a rotor speed of 31 rpm. The data was collected with the Mod-0

wind turbine stabilized in free yaw and depict a free yaw alignment angle. The nacelle yaw angle versus reference wind speed and wind speed distribution shown in figure 14(a), is similar in nature to the free yaw data taken for the fixed pitch twisted aluminum blades, and shows a fairly constant yaw angle which is relatively independent of the wind speed for the wind speed range of 4-14 m/s. Figure 14(b) depicts the probability density of the nacelle yaw angles and indicates the wind turbine stabilized in free yaw with steel spar blades, and tip control has a modal yaw angle of -46.5° .

The nacelle directional responses for the wind turbine in free yaw with the untwisted steel spar blades with tip control and at 31 rpm are shown in figures 15 and 16. As stated earlier, care should be taken in directly using the nacelle wind speed and nacelle yaw angle shown on these strip charts because of the possible nacelle/rotor interference. The nacelle was placed in free yaw at approximately -35° yaw angle and shows the tendency to reach and stabilize at the free yaw alignment angle. Unlike the rotor with twisted aluminum blades, the nacelle's motion as shown by the nacelle's azimuth is not clearly asymptotic nor as well damped. The "low dampened" yaw motion of the nacelle continues to occur at a "stabilized" nacelle free yaw alignment as shown in figure 16 where the wind turbine has been in free yaw for a long period of time (20 minutes). This figure does, however, indicate the nacelle yaw is dampened to short term variations in wind direction of $+10^{\circ}$ in 10 seconds.

Alternator power of the wind turbine in free yaw with untwisted steel spar blades and tip control was recorded for a nominal rotor speed of 31 rpm after the wind turbine had reached free yaw alignment. For this test a 2 speed high slip induction generator was used with no fluid coupling between the gear box and generator. It was set in the high speed mode and the maximum power was set at 90 kW. Drive train slip was measured to be 4% at rated power of 100 kW. The alternator power output for the wind turbine at free yaw alignment is presented in figure 17. The alternator power output of the same wind turbine in active yaw aligned with the wind is also given for comparison. The differences in power for the wind turbine in free yaw at approximately -48° yaw as compared to active yaw at 0° is readily apparent. The wind turbine in free yaw did reach the same maximum (limit) power output as the wind turbine aligned with the wind, however, at a wind speed 3 m/s higher. Power for the two configurations and at the prevalent wind speeds along with the median free yaw angle are tabulated in table 4. Again, simple power ratio of the wind turbine into the wind to the wind turbine in free yaw as a function yaw angle could be determined that was consistent with the data.

TABLE 4 - WIND TURBINE PERFORMANCE - FREE YAW VS. ACTIVE YAW
 INTO THE WIND - STEEL SPAR BLADES WITH TIP CONTROL
 AT 31 RPM

REF. WIND SPEED (m/s)	AT POWER- FREE YAW (kW)	YAW ANGLE- FREE YAW (DEG.)	ALT. POWER ACTIVE YAW (kW)
5.9	5.7	-49	39.0
6.9	18.4	-50	65.1
7.9	29.9	-50	98.0
8.9	49.0	-47	102.1

Analysis

An analysis was made of the predicted free yaw behavior of Mod-0 using the MOSTAB-HFW (MOdular STABility - High Frequency Wind) code. This code is a wind turbine version of a rotorcraft code also called MOSTAB-HFW developed for Air Systems Command (ref 8). In HFW, each rotor blade may be modelled with up to four aeroelastic degrees of freedom and the rotor hub may include teetering. The support for the rotor, however, is assumed to be rigid. Further details of the MOSTAB-HFW code are given in reference 9. The assumed blade distributed properties used to model the Mod-0 having 8-1/2° tilt with twisted aluminum blades described earlier and at 26 rpm are given in Appendix A.

The MOSTAB program predictions of the free yaw alignment angle for the Mod-0 wind turbine, with 8-1/2° nacelle tilt, having teetered fixed pitch twisted aluminum blades, 0° coning and at 26 rpm, were verified with data taken on Mod-0 wind turbine. To determine free yaw alignment, nacelle yaw torques were calculated for various trim yaw angles at wind speeds from 5-9 m/s. Since at free yaw alignment the sum of the yaw torques for the nacelle should be zero, a plot of yaw torques vs. yaw angles should indicate the free yaw alignment at zero yaw torque. With the yaw drive disconnected by a clutch and brake pressure set to 0 PSI, the yaw torques acting would be the torques generated by the rotor and friction torque. The rotor torques were computed by MOSTAB. The friction torque was estimated from experimental data to be 1900 N-M, based on nacelle weight of 1421 kilograms, friction coefficient of .02 and a yaw bearing radius of .69 meters. Figure 18 shows the yaw torques at various yaw angles calculated by MOSTAB for the given wind speed envelope. Also shown is the estimated yaw friction torque. The yaw equilibrium where the sum of the torques are zero and free yaw alignment occurs would be the range of yaw angles where the yaw friction torque intersects MOSTAB's nacelle yaw torque envelope, Figure 18 indicates a range of yaw angles of -55° to -35° where yaw equilibrium may occur depending upon the wind speed. The experimental free yaw alignment of -53.6° falls in that range. Considering the accuracy of the

estimated yaw friction and unsteady meteorological variables in the experimental data, the MOSTAB program predicts reasonably well wind turbine free yaw alignment.

Studies were made with the MOSTAB-HFW code to determine the effects of nacelle tilt, rotor coning and wind shear on wind turbine free yaw alignment. For these cases, a baseline wind turbine configuration was modeled and then one specific characteristic was changed. The resulting values of yaw torque were then compared to the baseline configuration yaw torque values. The baseline model used was the Mod-0 100 kW wind turbine with 8-1/2° nacelle tilt, teetered rotor with 0° coning, and fixed pitch twisted aluminum blades operating at 26 rpm in steady 7 m/s wind speeds. The effect of removing the 8-1/2° of nacelle tilt is shown in figure 19. The MOSTAB calculations show a positive shift of the yaw torque vs. yaw angle curve which indicates the nacelle will align closer to the wind of nacelle tilt is removed. A significant positive shift of the yaw torque vs. yaw angle curve was calculated by MOSTAB for the wind turbine with 7° coning as compared to the baseline wind turbine without coning, as shown in Figure 20. The addition of coning to the baseline model would cause the wind turbine to align closer with the wind. The effect of removing wind shear upon predicted yaw torque vs. yaw angle is small as shown in Figure 21. However, it indicates the wind shear does contribute to the off wind alignment of the wind turbine in free yaw.

CONCLUSIONS

Free yaw operation of the NASA Mod-0 wind turbine with 8-1/2° nacelle tilt and 0° coning and using both fixed pitch twisted blades and untwisted tip controlled blades resulted in the following conclusions:

1. The wind turbine is stable and damped in free yaw and readily seeks and maintains free yaw alignment at some yaw angle.
2. For the Mod-0 wind turbine configuration with 8-1/2° nacelle tilt, free yaw alignment was between -55° and -45° and independent of wind speeds between 5-9 m/s. The large off wind alignment of the nacelle, is believed to be mostly due to the nacelle tilt.
3. At these yaw angles power output of the wind turbine was reduced 30% to 50% from the power output of the wind turbine aligned with the wind.
4. Free yaw operation with twisted aluminum blades provided slightly more nacelle yaw damping than operation with untwisted steel spar blades with tip control.
5. MOSTAB predictions of free yaw alignment and rotor power correlated reasonably well with experimental data in the case of the Mod-0 wind turbine with twisted aluminum blades at 26 rpm.

6. MOSTAB calculations indicate that both removing tilt and adding coning will cause the Mod-0 wind turbine with teetered, fixed pitch, twisted aluminum blades to align closer to the wind.
7. Wind shear variations have a small affect on free yaw alignment, the less wind shear, the closer alignment to the wind.

REFERENCES

1. Puthoff, R. L.: Fabrication and Assembly of the ERDA/NASA 100-kW Experimental Wind Turbine. NASA TM X-3390, 1976.
2. Glasgow, J. C. and Birchenough, A. G.: Design and Operating Experience on the U.S. Department of Energy Experimental Mod-0 100-kW Wind Turbine. DOE/NASA/1028-78/18, NASA TM-78915, 1978.
3. Winemiller, J. R.; et al.: Design, Fabrication and Initial Test of a Fixture for Reducing the Natural Frequency of the Mod-0 Wind Turbine Tower. DOE/NASA 1028-79/24, NASA TM-79200, 1979.
4. Neustadter, H. E. and Spera, D. A.: Applications of the DOE/NASA Wind Turbine Engineering Information System. Paper presented at the Second DOE/NASA Wind Turbine Dynamics Workshop, Cleveland, Ohio, Feb. 24-26, 1981.
5. Henninger, William C.; Hoffman, John A.; and Williamson, Dale R.: Mathematical Methods Incorporated in the Wind Energy System Coupled Dynamics Analysis: Part I - Basic Methodology for the Modular Stability Derivative Program (Revision B); Part II - Analysis Methods Incorporated in the MOSTAB-HFW Computer Code; Part III - Methodology: Wind Turbine Linear Analysis Software System (WINDLASS). PPI-1014-7, Paragon Pacific, Inc., January, 1977.
6. Henninger, William C.; Hoffman, John A.; and Williamson, Dale R.: MOSTAS User's Manual: Volume I - User's Manual for the Modular Stability Derivative Program - High Frequency Wind Turbine Version (MOSTAB-HFW), PPI-1014-8, Volume II - User's Manual for the Wind Turbine Linear Analysis Software System (WINDLASS), PPI-1014-9. Paragon Pacific, Inc., January, 1977.
7. Hoffman, J. A.: Coupled Dynamics Analysis of Wind Energy Systems. NASA CR 135152, 1977.
8. Hoffman, John A.: Analysis Methods Incorporated in the MOSTAB-HFA Computer Code. PPI-1013-2, Paragon Pacific, Inc., 1975.
9. Williamson, Dale R.: Design of Articulated Hub Concepts. PPI-1014-10, Vols. I and II, Paragon Pacific, Inc., 1977.

ORIGINAL PAGE IS
OF POOR QUALITY

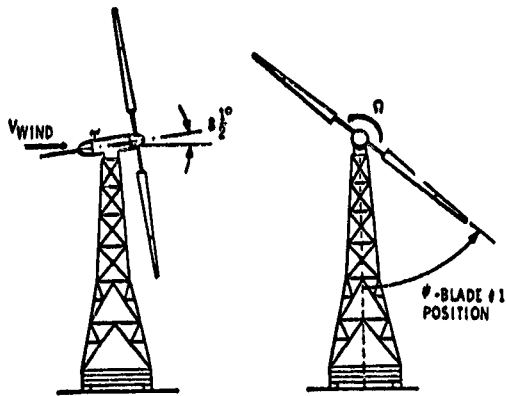


FIGURE 1. NASA MOD-0 WIND TURBINE

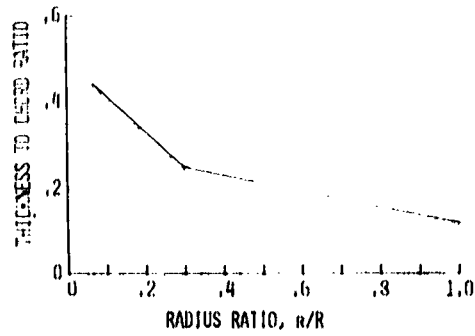


FIG. 4. THICKNESS TO CHORD RATIO
FOR TWISTED ALUMINUM BLADE.

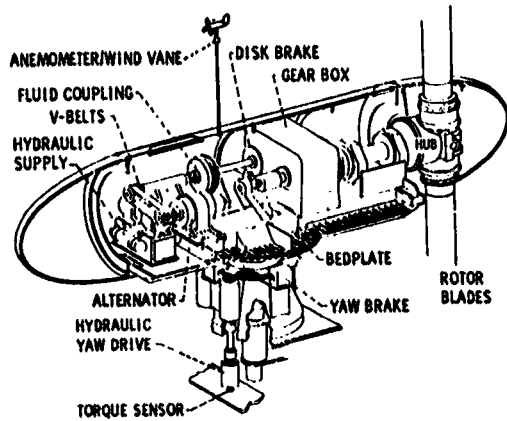


FIGURE 2. NASA MOD-0 WIND TURBINE NACELLE
INTERIOR WITH TEETERED HUB

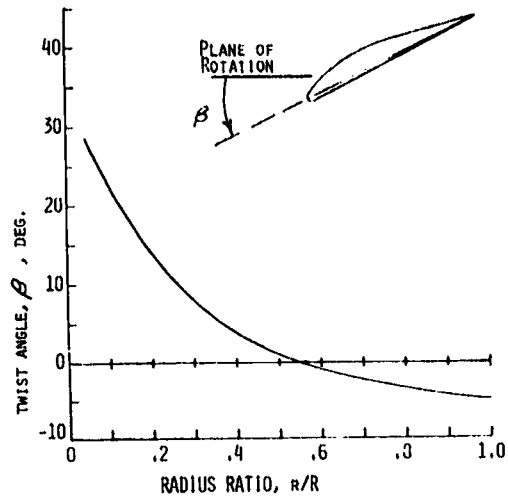


FIG. 5. TWIST DISTRIBUTION FOR
TWISTED ALUMINUM BLADES.

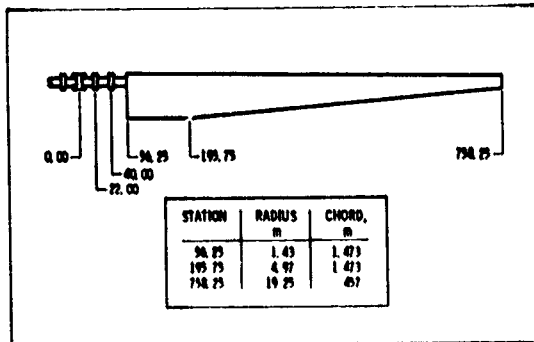


FIG. 3. BLADE PLANFORM TWISTED
ALUMINUM BLADES

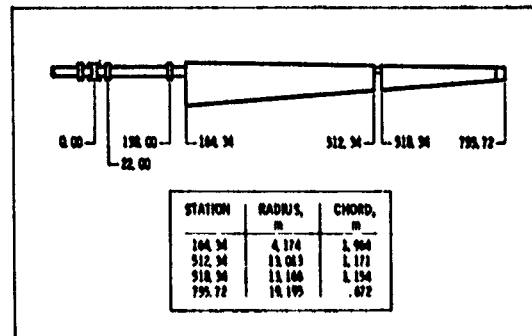


FIG. 6. BLADE PLANFORM - STEEL
SPAR WITH TIP CONTROL BLADES

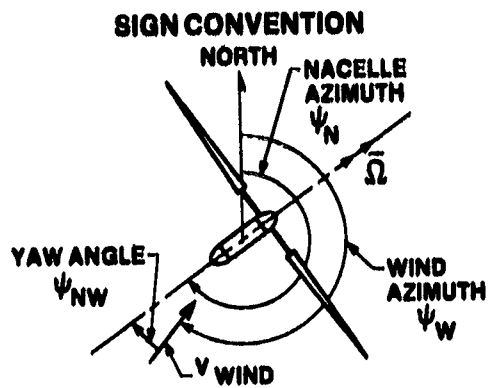


FIGURE 7. MOD-0 NACELLE YAW POSITION SIGN CONVENTIONS

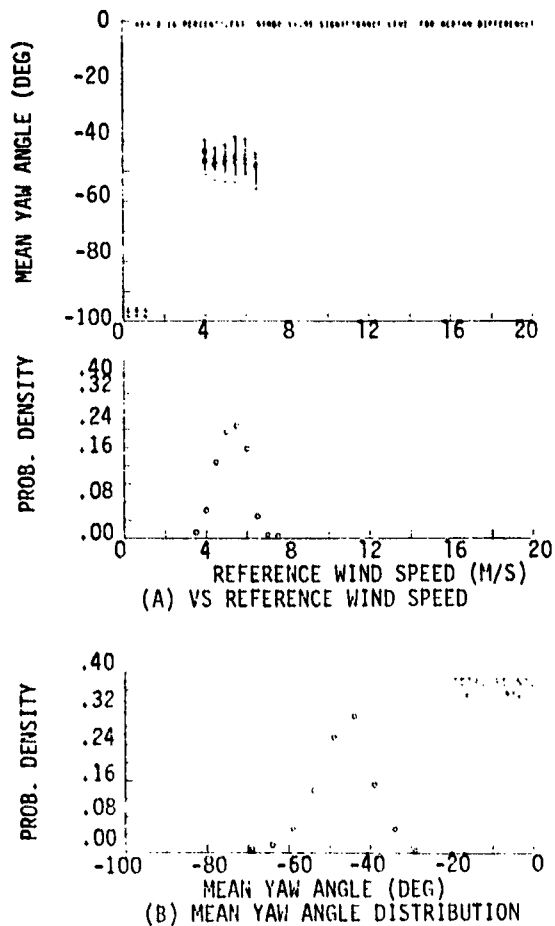


FIG. 8. FREE YAW ALIGNMENT DATA FOR WT WITH TWISTED BLADES AT 20 RPM VS. REFERENCE WIND SPEED (A), AND DISTRIBUTION (B).

ORIGINAL PAGE IS OF POOR QUALITY

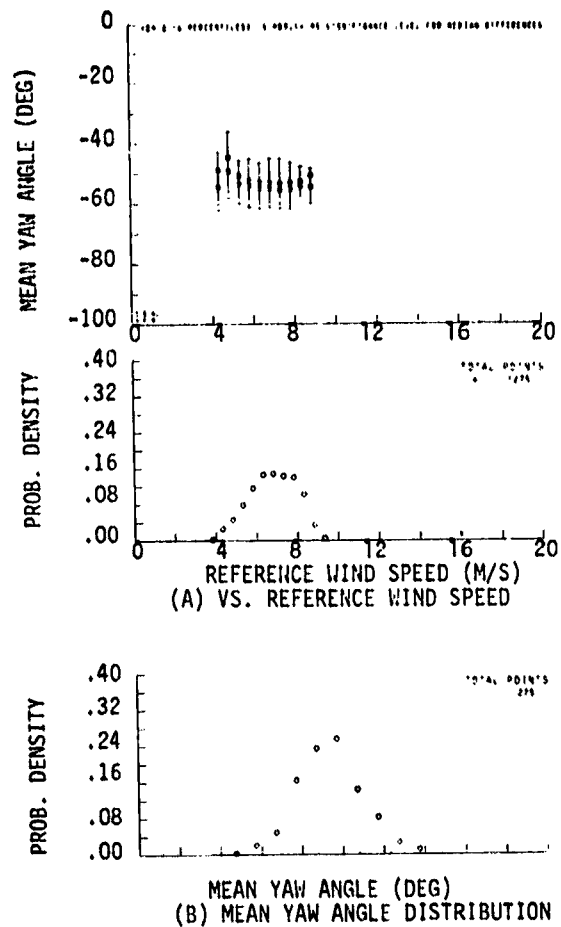


FIG. 9. FREE YAW ALIGNMENT DATA FOR WT WITH TWISTED BLADES AT 26 RPM VS. REFERENCE WIND SPEED (A), AND DISTRIBUTION (B).

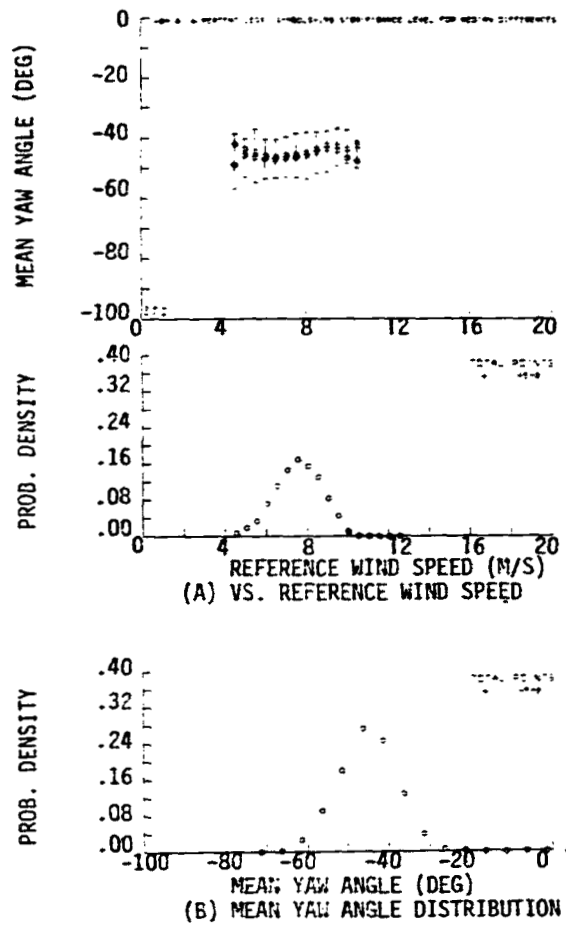


FIG. 10. FREE YAW ALIGNMENT OF WT WITH TWISTED BLADES AT 31 RPM VS. REFERENCE WIND SPEED (A) AND DISTRIBUTION (B).

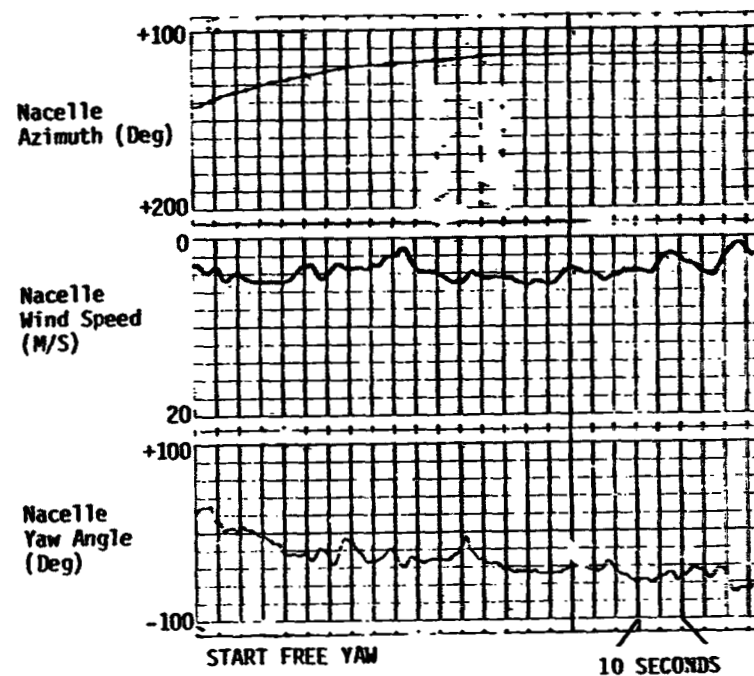


FIG. 11. STRIP CHART RECORDING OF WT WITH TWISTED ALUMINUM BLADES AT 26 RPM PLACED IN FREE YAW AT 0° YAW ANGLE.

ORIGINAL PAGE IS
OF POOR QUALITY

ORIGINAL PAGE IS
OF POOR QUALITY

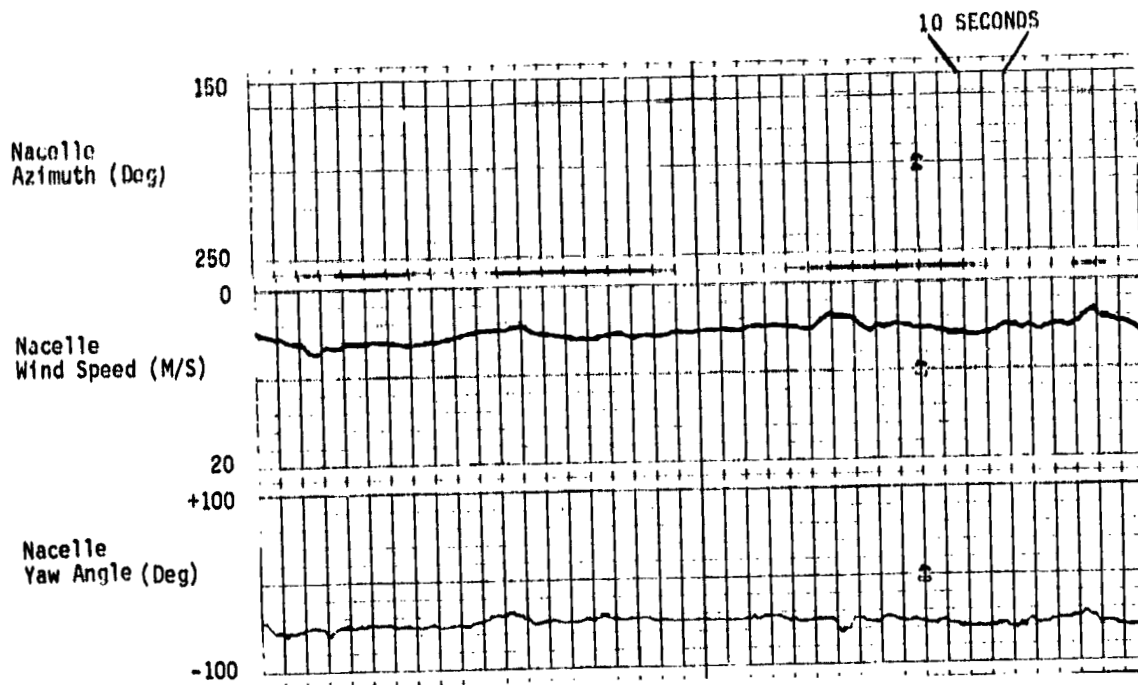


FIG. 12. STRIP CHART RECORDING
OF WT WITH TWISTED BLADES AT
26 RPM STABILIZED AT FREE YAW
ALIGNMENT.

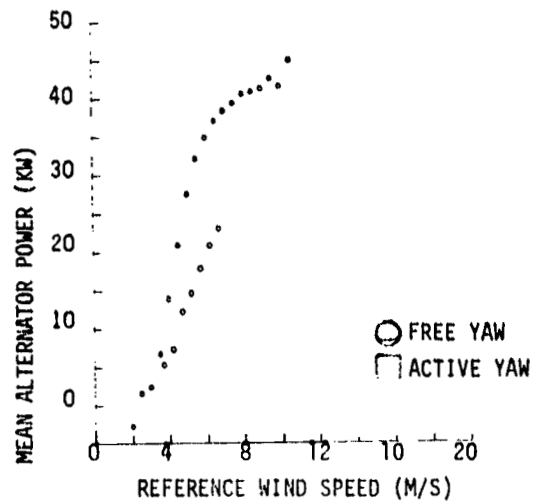


FIG. 13. MEAN ALTERNATOR POWER
VS. REFERENCE WIND SPEED FOR WT
WITH TWISTED ALUMINUM BLADES AT
20 RPM FOR BOTH FREE YAW AND
ACTIVE YAW INTO THE WIND.

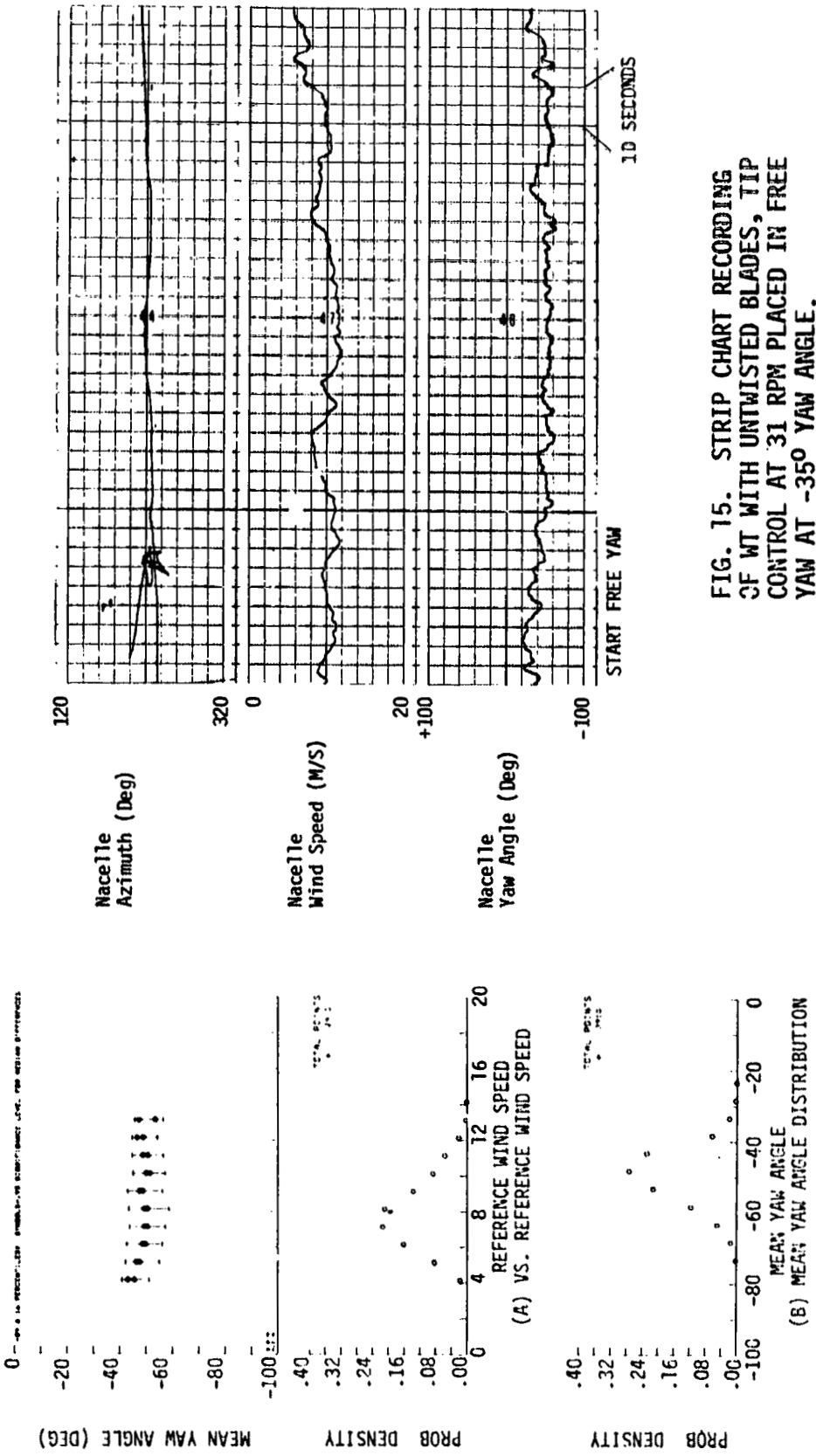


FIG. 15. STRIP CHART RECORDING
OF WT WITH UNTWISTED BLADES, TIP
CONTROL AT 31 RPM PLACED IN FREE
YAW AT -35° YAW ANGLE.

FIG. 14. FREE YAW ALIGNMENT OF
WT WITH UNTWISTED BLADES, TIP
CONTROL AT 31 RPM VS. REFERENCE
WIND SPEED (A) AND DISTRIBUTION (B).

ORIGINAL PAGE IS
OF POOR QUALITY

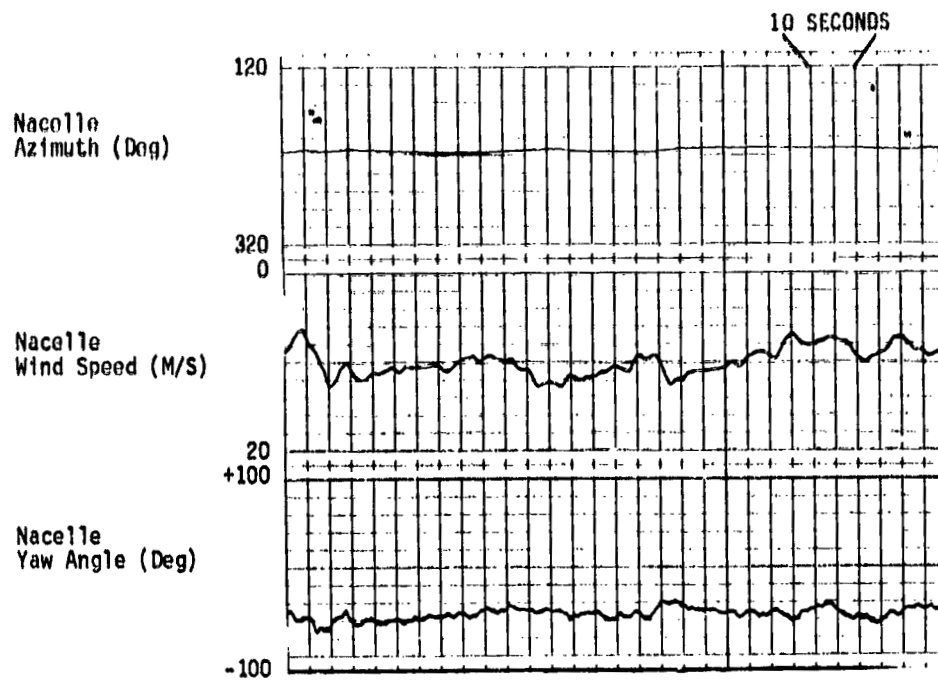


FIG. 16. STRIP CHART RECORDING
OF WT WITH UNTWISTED BLADES, TIP
CONTROL AT 31 RPM STABILIZED AT
FREE YAW ALIGNMENT.

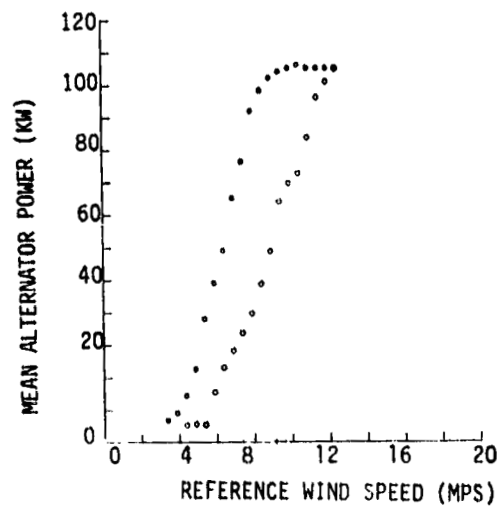


FIG. 17. MEDIAN ALTERNATOR POWER
VS. REFERENCE WIND SPEED FOR WT
WITH UNTWISTED BLADES, TIP
CONTROL AT 31 RPM IN FREE YAW
AND ACTIVE YAW INTO THE WIND

ORIGINAL PAGE IS
OF POOR QUALITY

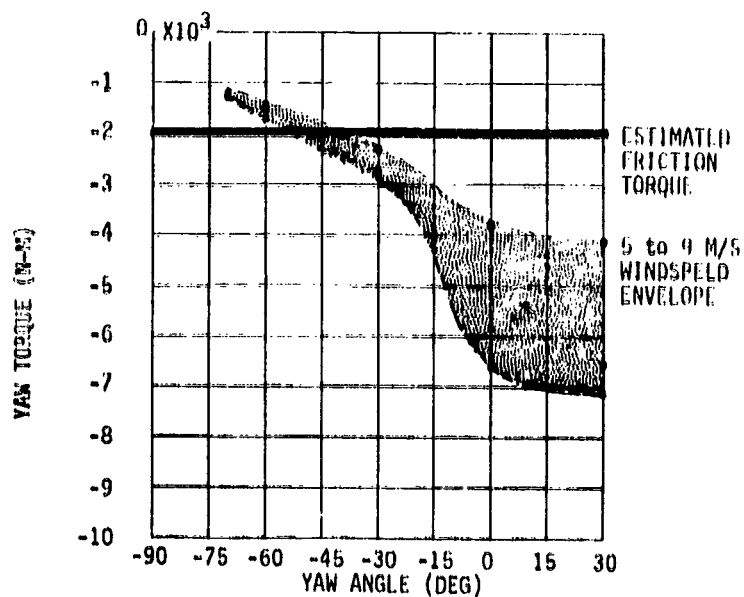


FIG. 18. MOSTAB COMPUTED YAW TORQUE ENVELOPE FOR MOD-0 AT 26 RPM.

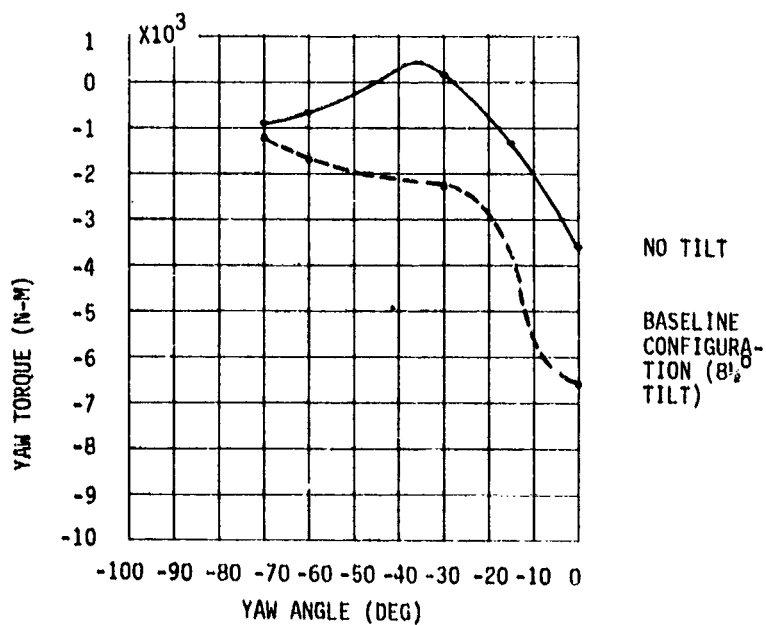


FIG. 19. MOSTAB COMPUTED EFFECTS OF TILT ON YAW TORQUES FOR MOD-0 AT 26 RPM IN 7 M/S WINDS.

ORIGINAL PAGE IS
OF POOR QUALITY

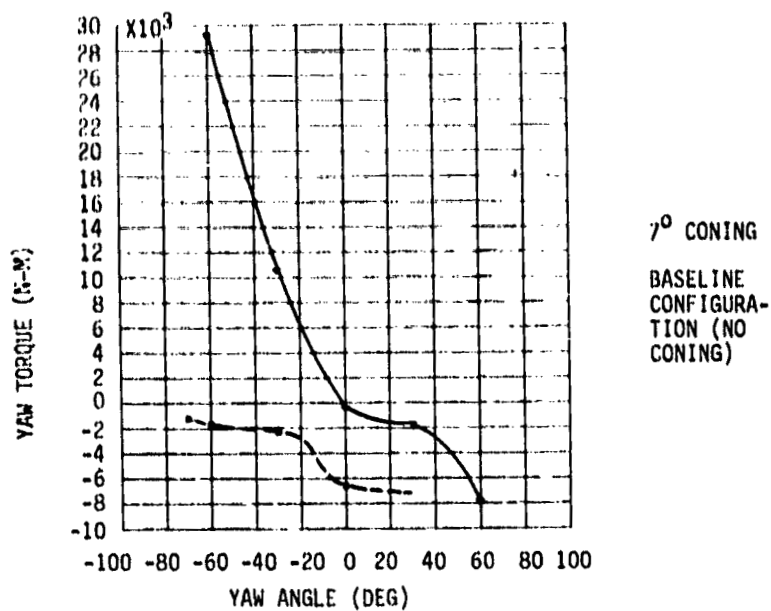


FIG. 20. MOSTAB COMPUTED CONING EFFECT ON YAW TORQUES FOR MOD-O WT AT 26 RPM IN 7 M/S WIND.

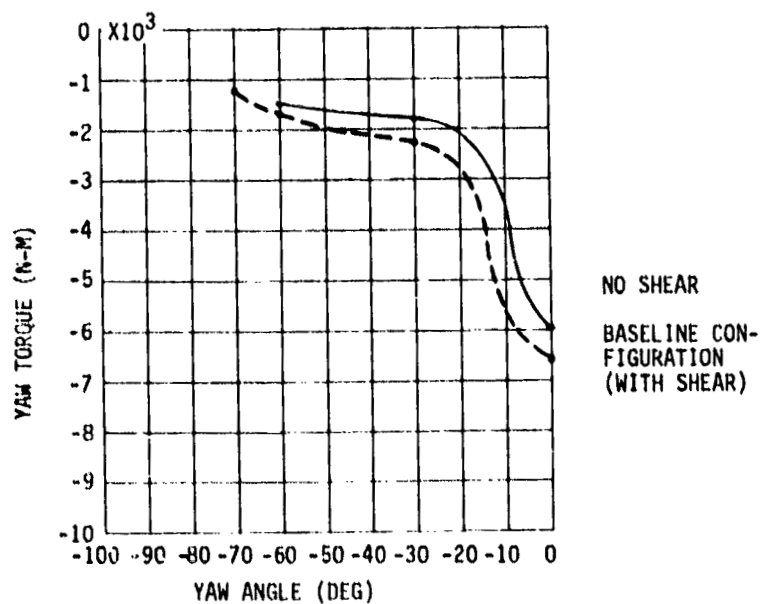


FIG. 21. MOSTAB COMPUTED EFFECT OF SHEAR TORQUES FOR MOD-O WT AT 26 RPM IN 7 M/S WINDS

ORIGINAL PAGE 13
OF POOR QUALITY

APPENDIX A

MOSTAB INPUT MODEL OF THE MOD-0 WIND TURBINE
HAVING 8.5° NACELLE TILT, NO ROTOR CONING AND
TWISTED FIXED PITCH ALUMINUM BLADES OPERATING
AT A ROTOR SPEED OF 26 RPM.

MZTP	MOSTAB-HFW	MOD-0 WITH TEETERED HUB		
.0000	.0000	.0000	.0000	.0000
GIMBAL DATA				
.1000+001	.0000	.0000	.0000	.0000
.0000	.0000	.0000	.0000	.0000

DISTRIBUTED BLADE PROPERTIES FOR AEROELASTIC ROTOR ANALYSIS

STATION	S FT	MASS SLUGS/FT	CHORD FT	YCG	ZCG	INERTIA TENSORS		
						IYY	IYZ	IZZ
1	.00	.00000	.0000	.000	.000	.000	.000	.000
2	3.33	.00000	.0000	.000	.000	.000	.000	.000
3	4.70	.00000	4.5000	.000	.000	.000	.000	.000
4	6.75	1.02400	4.5000	-.139+000	.000	.103+001	.638-001	.161+001
5	15.63	1.07800	4.5000	-.192+000	.000	.213+000	.220+000	.101+001
6	29.00	1.33900	3.9250	.575-001	.000	.110+000	.109-001	.024+000
7	30.83	1.15200	3.5575	.000	.000	.040-001	.900-002	.702+000
8	37.50	.94620	3.1375	.000	.000	.400-001	.487-002	.424+000
9	46.88	.69590	2.5469	.000	.000	.154-001	.106-002	.239+000
10	50.00	.65290	2.3500	.000	.000	.047-002	.190-002	.176+000
11	56.25	.34640	1.9562	.000	.000	.191-002	.741-003	.625-001
12	59.38	.32570	1.7594	.000	.000	.191-002	.741-003	.625-001
13	62.50	.29040	1.5625	.000	.000	.047-003	.318-003	.477-001

CONCENTRATED MASS PROPERTIES FOR AEROELASTIC ROTOR ANALYSIS

STATION	S FT	MASS SLUGS	YCG	ZCG	IYY	IYZ	IZZ
1	3.33	.094+001	.000	.000	.496+000	.000	.496+000
2	5.37	.850+001	.000	.000	.133+001	.159-002	.246+001
3	1.00	.140+002	.000	.330+000	.305+002	.000	.305+002

ORIGINAL PAGE 13
OF POOR QUALITY

MZTR MOSTAB-HFW MOD-D WITH TEETERED HUB

STATION	S	INITIAL SHAPE FUNCTIONS -		TWIST, RAD			
		SWG(2)	SWG(3)	SWG(4)	SWG(2)	SWG(3)	SWG(4)
1	FT	.000	.000	.000	.000	.000	-.100+001
2	3.33	.000	.000	.000	.000	.000	-.100+001
3	4.00	.000	.000	.556+000	.000	.000	-.100+001
4	6.75	.000	.000	.586+000	.000	.000	-.100+001
5	15.63	.000	.000	.261+000	.000	.000	-.100+001
6	25.00	.000	.000	.119+000	.000	.000	-.100+001
7	30.83	.000	.000	.715-001	.000	.000	-.100+001
8	37.50	.000	.000	.346-001	.000	.000	-.100+001
9	46.88	.000	.000	.000	.000	.000	-.100+001
10	50.00	.000	.000	-.870-002	.000	.000	-.100+001
11	56.25	.000	.000	-.233-001	.000	.000	-.100+001
12	59.38	.000	.000	-.294-001	.000	.000	-.100+001
13	62.50	.000	.000	-.349-001	.000	.000	-.100+001

MODAL DATA-

MODE NO. 1 OMEGA = 11.56970	MODE NO. 2 OMEGA = 15.92200
BETA E = .0000	BETA E = .0000
BETADOT E = .0000	BETADOT E = .0000
INTEGRATION SPECIFICATION = 1.0000	INTEGRATION SPECIFICATION = 1.0000
ZETA = .0000	ZETA = .0000

STATION	S	DEL(2)	DEL(3)	DEL(4)	DEL(2)	DEL(3)	DEL(4)
1	.00	.00000	.00000	.00000	.00000	.00000	.00000
2	3.33	.00240	-.01110	.00000	-.04150	-.00640	.00000
3	4.00	.00450	-.02100	.00000	-.07770	-.01200	.00000
4	6.75	.02180	-.09880	.00000	-.35580	-.04970	.00000
5	15.63	.19140	-.77790	.00000	-2.34370	-.19660	.00000
6	25.00	.59240	-2.48240	.00000	-6.31330	-.50920	.00000
7	30.83	.94570	-4.18330	.00000	-9.66140	-.90970	.00000
8	37.50	1.42020	-6.75450	.00000	-14.16380	-1.65450	.00000
9	46.88	2.10440	-11.74450	.00000	-21.58420	-3.48990	.00000
10	50.00	2.45750	-13.85820	.00000	-24.34090	-4.40380	.00000
11	56.25	3.01710	-18.83740	.00000	-30.24520	-6.80610	.00000
12	59.38	3.29280	-21.84340	.00000	-33.33690	-8.43130	.00000
13	62.50	3.56730	-24.94460	.00000	-36.45700	-10.14320	.00000